Strojniški vestnik - Journal of Mechanical Engineering 67(2021)5, 223-234
DOI:10.5545/sv-jme.2021.7089
Original Scientific Paper
Received for review: 2021-01-05
Received revised form: 2021-04-20
Accepted for publication: 2021-05-03

Investigation on the Modeling and Dynamic Characteristics of a Novel Hydraulic Proportional Valve Driven by a Voice Coil Motor

Mingxing Han[1,*] – Yinshui Liu[2] – Yitao Liao[1] – Shucai Wang[1]
[1]Huazhong Agricultural University, College of Engineering, China
[2]Huazhong University of Science and Technology, School of Mechanical Science and Engineering, China

As the key control component of the water hydraulic systems, the water hydraulic proportional valve has a significant influence on the control performance of the systems. Due to the poor viscosity and lubricity of water, the valve spool resistance is large and non-linear. In this study, a novel fast-response water hydraulic proportional valve is presented. The actuator of the valve adopts a voice coil motor (VCM), which has the advantages of fast response, high control precision and small volume. In order to realize the fast control of the valve, a lever amplifier is designed to obtain enough actuation force. A detailed and precise non-linear mathematical model of the valve considering both the valve's structural parameters and VCM electromagnetic characteristics is developed. A comprehensive performance simulation analysis has been carried out, mainly divided into an electromagnetic simulation, an analysis of the characteristics of the lever magnifier, and a dynamic performance simulation of the valve. The simulation results show that the adjusting time is about 28 ms, and the maximum overshoot is about 5 %. The step response rise time is about 15 ms. The test rig of the valve and VCM have been built. The test results of the prototype show that the optimal stroke range of VCM is 4 mm to 15 mm. The maximum overshoot of the valve is around 10 %; the adjusting time is about 30 ms in the opening process and 35 ms in the closing process. The test results prove that the valve has good static and dynamic control performance.
Keywords: proportional control valve, voice coil motor, optimization design, dynamic performance

Highlights
- *A novel water hydraulic proportional valve with fast response is proposed.*
- *The actuator of the valve adopts a voice coil motor (VCM), and a lever amplifier is designed to obtain enough actuation force to realize the fast and accurate control.*
- *The detailed and precise mathematical models of the valve have been developed, and the comprehensive optimization design has been carried out.*
- *The test rig has been built, and the results indicate that the step response time of 0 % to 100 % stroke is about 30 ms.*

0 INTRODUCTION

Compared with oil hydraulic systems, water hydraulic systems could be a good solution for the environmental and safety problems [1]. Water hydraulic systems are widely used in steel and glass production, ocean exploration, food and medicine processing, and coal mining [2] to [4]. The water hydraulic control valve is one of the most important components of hydraulic systems, and its dynamic performance has an important impact on the performance of hydraulic systems [5]. However, it is quite difficult to design a high-performance water hydraulic proportional valve due to the low viscosity and oxidative corrosion of water. Many problems, such as poor lubrication and large friction, sealing, and leakage, need to be solved in the design process. Some studies [6] have shown that while the oil directional control sliding valve worked perfectly, there is a strengthening oscillatory movement of the same water valve spool, caused by non-optimal valve material combination (steel/steel) in water-lubricated conditions.

The current research indicates that the dynamic performance of electro-mechanical devices is one of the key factors affecting the response speed of the control valve [7]. Considering that the high-speed on/off solenoids have fast response, some water hydraulic control valves are designed with them as the actuators [8] and [9]. However, they are usually used in high-speed switching valves with small flow capacity due to the small actuation force and stroke. Park et al. [10] and Park [11] proposed a water pressure proportional valve with the high-speed switching valve as a pilot stage, and the experiments show that the maximum flow rate can reach 9 l/min and the pressure drop is 7 MPa. This kind of valve can realize proportional control by pulse width modulation (PWM) signal but cannot achieve a good control effect. Piezoelectric actuators have become a solution for improving the valve dynamic performance because of their high response speed and high output force. However, their stroke usually is very small even at a large applied voltage, and the properties are greatly affected by temperature [12] and [13]. These drawbacks restrict

*Corr. Author's Address: College of Engineering, Huazhong Agricultural University, Wuhan, China, 430070. hanmingxing@mail.hzau.edu.cn

the valve opening (which in turn limits maximum flow rate), and it is difficult to adapt to the working environment. Compared with the high-speed on/off solenoids and piezoelectric actuators, a voice coil motor (VCM) has the obvious advantages of fast response and large stroke-actuation force. Therefore, as a high-performance actuator, a voice coil motor has attracted the attention of researchers. Dahoon et al. [14] designed a high force voice coil motor. VCM usually can provide 0.7 N to 1000 N actuation force and 0 mm to 100 mm stroke. The motion frequency of VCM can reach 1000 Hz. It is widely used in medical, aviation, vibration platform control, etc. A comparison of these existing electro-mechanical devices shows that VCM is an appropriate choice for electro-mechanical actuators in water hydraulic control valve.

As an ideal electric-mechanical conversion device, VCM can be used to quickly and accurately control the movement of the valve spool. Li et al. [15] and [16] proposed a pneumatic servo-valve with control pressure up to 20 MPa, which was driven by VCM. Experiments show that the valve has good control performance, and the step response frequency can reach 100 Hz. Zhang et al. [17] proposed a direct-drive water hydraulic control valve driven by a voice coil motor, and the rated flow is 14 l/min. The test results show that the control valve has the performance of approximate linear proportional control. In contrast, other researchers are committed to improving the dynamic performance of the valve by optimizing structural parameters. Liu et al. [18] studied a novel throttle poppet valve based on the hydraulic feedback principle. Filo et al. [19] proposed a novel control valve that consists of a throttle valve and a differential valve controlled by the pressure difference between the supply line and the return line to increase the speed of cylinder piston rod movement. Xu et al. [20] studied the mathematical modelling and simulation of a novel hydraulic variable valve time system. Simic and Herakovic [21] pointed out that non-optimized hydraulic valve geometry is the main cause for many problems related to response time, actuation force and energy consumption. The results of the simulation analyses show that the axial component of the flow forces could be reduced significantly by optimizing the geometry of the valve spool and housing.

Due to the poor viscosity and lubricity of the water medium, the conventional hydraulic valve structure and the optimization design method will be not suitable for the water hydraulic proportional valve. In this study, a novel fast-response water hydraulic proportional valve that driven by VCM is presented. A comprehensive performance simulation analysis has been carried out, which mainly includes electromagnetic simulation of VCM, characteristics analysis of lever magnifier and dynamic performance simulation of the valve.

1 STRUCTURE AND PRINCIPLE OF THE VALVE

The water hydraulic valve proposed in this study uses a lever amplifier to amplify the VCM actuation force (as shown in Fig. 1). A smaller VCM can be used to drive the spool to move quickly. The traditional oil hydraulic control valve mostly adopts the slide valve structure. Due to its small sealing clearance, the working fluid cleanliness level has a significant impact on the valve performance [22]. The existing research shows that water hydraulic control valve with non-gap sealing structures, such as the seat valve (ball valve, disc valve, poppet valve etc.), can effectively solve the leakage problem caused by the low viscosity of water and improve the anti-pollution ability of the valve. The valve orifice adopts a seat valve structure, which is mainly composed of seat and ball. The displacement sensor detects the spool position, and the displacement signal will be fed back to the PID controller for closed-loop control.

The water hydraulic control valve with non-gap sealing structures such as seat valve (ball valve, disc

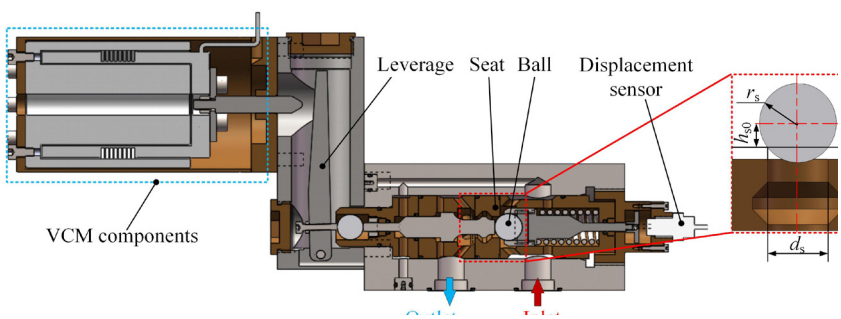

Fig. 1. *Structure of the water hydraulic proportional valve*

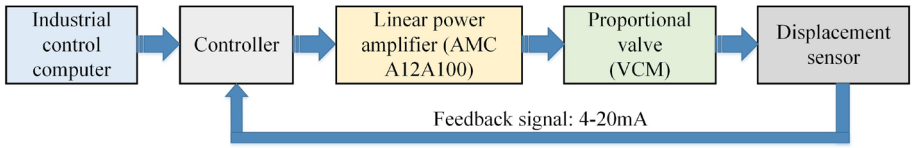

Fig. 2. *The valve control schematic*

valve, poppet valve etc.) can effectively solve the leakage problem caused by the low viscosity of water and high working pressure [7] and [11]. The valve orifice adopts a seat valve structure, which is mainly composed of valve seat and ball. The displacement sensor detects the spool position, and the displacement signal will be fed back to the controller for closed-loop control. The main parameters of the prototype are shown in Table 1.

Table 1. *The main parameters of the valve*

Parameter	Symbol	Value	unit
Fluid density	ρ	1000	kg/m³
Flow coefficient	C_d	0.82	/
Valve seat diameter	d_s	10	mm
Valve ball diameter	r_s	12.7	mm
Return spring stiffness	k_{sv}	18	N/mm
Valve opening	x_v	0 to 1.2	mm

The closed-loop control has been used to improve the control precision and anti-interference ability of the valve. The control schematic is shown in Fig. 2. The control system is composed of a PC, controller, linear power amplifier (linear motor driver, AMC A12A100), displacement sensor and the water hydraulic proportional valve, etc. The PC sends out the control command, and the controller compares the control command with the feedback displacement signal. Through the comparison operations, ±10V control signal will be output to the VCM linear driver (AMC A12A100). The linear driver linearly amplifies the control signal into 0 A to 10 A current to drive VCM so as to drive the spool to move until reaching the specified position. At that point, the valve spool is finally kept at the specified position.

2 THE VALVE MODEL

As the intermediate structure of transfer force and displacement, the lever amplifier significantly influences the performance of the valve. Based on the VCM model and the valve model, the influence of lever amplifier parameters on the dynamic performance is studied in detail.

2.1 VCM model

Fig. 3 shows the principle of VCM, and Table 2 shows the main VCM parameters. It is composed of the support, coil, magnet yoke, soft iron and permanent magnet. The real permanent magnetic material and soft iron material are N40H and DT3, respectively. The permanent magnet provides a uniform and constant magnetic field inside the motor. According to Lorentz force law, the Lorentz force will be produced when the coil is electrified in the magnetic field. The Lorentz force is the actuation force for the VCM and drives the coil to move.

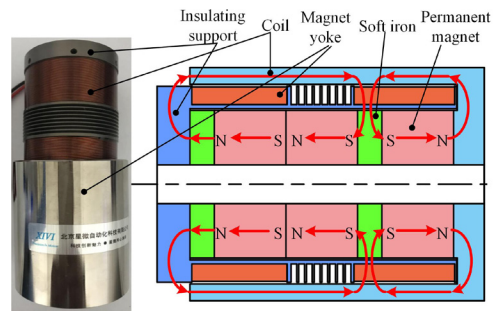

Fig. 3. *VCM composition and arrangement of internal magnetic poles*

The arrangement of the inner magnetic pole is shown in Fig. 3. A total of three permanent magnets are designed and installed in VCM. Among them, the two permanent magnet poles at the bottom are assembled in reverse to form a strong magnetic gathering effect at the working air gap. This will also help to reduce magnetic leakage and improve magnetic induction strength. Then the electromagnetic efficiency will be greatly improved.

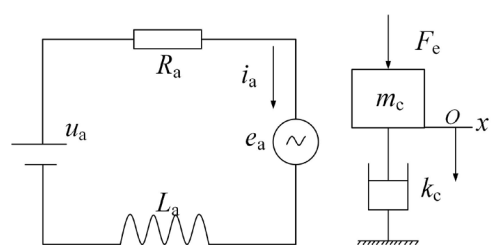

Fig. 4. *The VCM equivalent electrical circuit and equivalent dynamic model*

Table 2. *The main parameters of VCM*

Parameter	Value	unit
Maximum voltage	24.5	V
Maximum current	5.8	A
Continuous actuation force	51.5	N
Peak actuation force	160	N
Stroke	0 to 18	mm
Force constant	27.5	/

When the coil is electrified, Lorentz force will be produced and drive the coil to move. The dynamic model of VCM can be simplified as a mass damping mechanical motion system. Therefore, VCM can be equivalent to the coil equivalent circuit model and mass damping motion model, as shown in Fig. 4. According to the force balance equation and voltage balance equation of VCM, the mathematical model can be obtained as Eq. (1).

$$\begin{cases} F_e = B_\sigma l_c N i_a \\ u_a = e_a + i_a R_a + L_a \dfrac{di_a}{dt} \\ e_a = B_\sigma l_c \dot{x}_c \\ F_e = m_c \ddot{x}_c + k_c \dot{x}_c \end{cases}, \tag{1}$$

where F_e is the electromagnetic force of VCM [N]; k_c is the damping coefficient [N/(m/s)]; i_a is the current in the coil [A]; u_a is the voltage of the coil armature [V]; e_a is the back electromotive force generated by the coil motion [V]; L_a is the coil inductance [H]; m_c is the mass of the coil [kg].

2.2 Valve Dynamic Model

Compared with the poppet valve, the ball valve can realize a self-centring function. Therefore, it has better sealing performance than the poppet valve. In order to obtain good sealing performance, the valve adopts the structure of the ball valve. The flow rate of the valve can be calculated with the following equations:

$$\begin{cases} q_v = C_d A(x_v)\sqrt{\dfrac{2\Delta p_s}{\rho}} \\ A(x_v) = \pi d_s h_{s0} \dfrac{(1+\dfrac{x_v}{2h_{s0}})x_v}{\sqrt{\left(\dfrac{d_s}{2}\right)^2 + (h_{s0}+x_v)^2}} \end{cases}, \tag{2}$$

where C_d is flow coefficient of valve orifice; Δp_s is the pressure difference of the valve [MPa]; ρis the water density [kg/m³]; d_s is the diameter of the valve seat [m]; x_v is the valve opening [m]; h_{s0} can be calculated with the following formula:

$$h_{s0} = \sqrt{r_s^2 - \left(\frac{d_s}{2}\right)^2}. \tag{3}$$

When the spool is moving, the valve will be subjected to the comprehensive effect of flow force, spring force, friction force, inertia force, and viscous resistance (as shown in Fig. 5). VCM needs to provide enough driving force to overcome these resistances so that the valve spool has enough acceleration to meet the requirements of rapid response. Assuming that the opening direction of the valve is positive, the kinetic equation can be established as follows:

$$\begin{cases} m_s \ddot{x}_v = F_s + \dfrac{\pi p_s}{4}(d_2^2 - d_5^2) + \\ \qquad \dfrac{\pi p_k}{4}(d_5^2 - d_2^2) - F_{fl} - F_{fv1} - F_{ks1} \\ F_{ks1} = k_{sv}(l_{v0} + x_v) \\ F_{fl} = \sum 1.57 \mu_f d_i \sqrt{4r_o^2 - 0.25\Delta h^2}\,\Delta p_o \\ F_{fv1} = \rho q_v v \cos\alpha_0 \end{cases}, \tag{4}$$

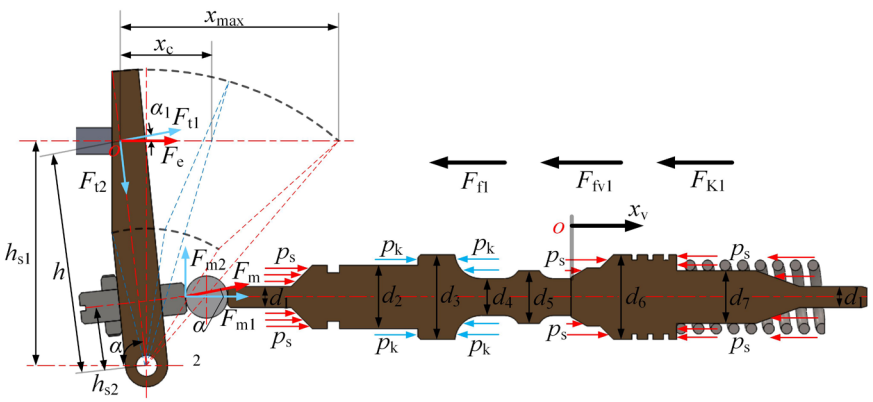

Fig. 5. *The force analysis of the valve*

where m_s is equivalent mass of the valve moving parts [kg]; p_s is the inlet pressure [MPa]; d_i is the diameter of the valve stem (i =1, 2, 3, 4, 5) [m]; p_k is the pressure acting on the stem (MPa); F_{fl} is the friction force [N]; F_{ks1} is then spring force [N]; F_{fv1} is flow force (N); k_{sv} is spring stiffness [N/m]; l_{v0} is initial compression of spring [m]; μ_f is the friction coefficient of o-ring; r_o is the o-ring radius [m]; Δh is O-ring compression [m]; Δp_o is difference pressure acting on o-ring [MPa]; q_v is the flow rate [l/min]; v is the valve orifice flow velocity [m/s]; α_0 is the valve orifice jet angle [°]. Where F_s is the driving force acting on the ball, and it can be got by:

$$F_s = \begin{cases} F_e \cos(\arctan(\cot\alpha - \frac{x_c}{h_{s1}}))\frac{h_{s1}}{h_{s2}} & x_c \le h_{s1}\cot\alpha \\ F_e \cos(\arctan(\frac{x_c}{h_{s1}} - \cot\alpha))\frac{h_{s1}}{h_{s2}} & x_c > h_{s1}\cot\alpha \end{cases}, \quad (5)$$

In the same way, the relationship between the stroke of VCM and the stroke of the valve spool can be obtained:

$$x_v = \begin{cases} \dfrac{x_c h_{s2}}{(\cos(\arctan(\cot\alpha - \frac{x}{h_{s1}}))h_{s1})} & x_c \le h_{s1}\cot\alpha \\ \dfrac{x_c h_{s2}}{(\cos(\arctan(\frac{x}{h_{s1}} - \cot\alpha))h_{s1})} & x_c > h_{s1}\cot\alpha \end{cases}, \quad (6)$$

where F_e is Lorentz force of VCM [N]; α is the swing angle of leverage [°]; h_{s1} is the centre distance of VCM [m]; h_{s2} is the centre distance of ball [m]; x_c is the coil displacement [m].

3 SIMULATION ANALYSIS

Based on the mathematical model of the valve, the simulation model can be established in the MATLAB/Simulink and Maxwell 3D, respectively. The influence of the lever parameters on the performance of the output actuation force and displacement is compared and analysed, following which the best amplification coefficient is obtained.

3.1 Electromagnetic Simulation

The simulation model of VCM is established in Maxwell 3D, as shown in Fig. 6. Since the VCM is of symmetrical structure, half of the model can be used for simulation calculation to improve the calculation efficiency. The main electromagnetic simulation parameters of VCM is shown in Table 3.

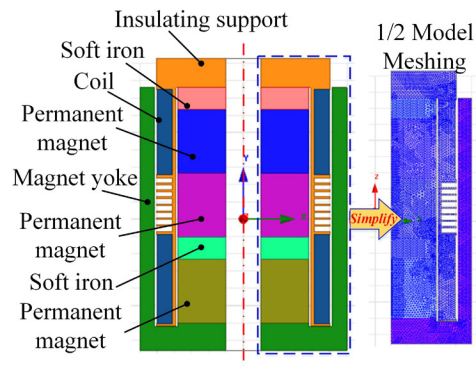

Fig. 6. *VCM FEM model*

Table 3. *Electromagnetic simulation parameters*

Name	Soft iron	Permanent magnet	Coil
Para-meter	Material: 10#	Material: N40H; Coercivity: 970 kA/m; Remanence: 1.3 mT	Copper wire diameter:0.5 mm; Turns - number: 550; Inside diameter of coil:41 mm; Outside diameter of coil:50 mm; Coil length:50.6 mm

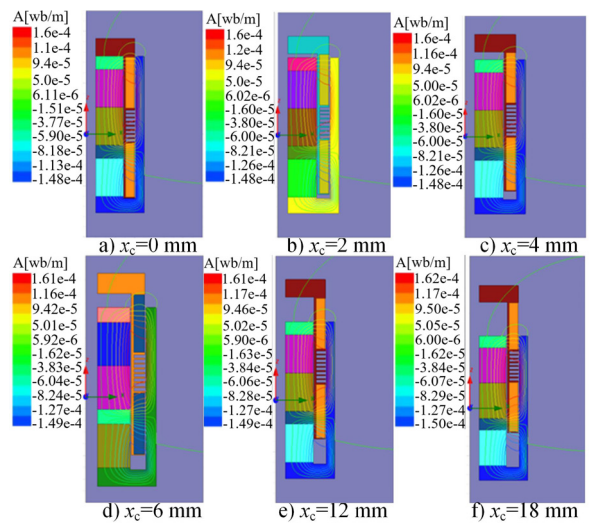

Fig. 7. *Electromagnetic simulation of VCM in the whole stroke, a) x_c = 0 mm, b) x_c = 2 mm, c) x_c = 4 mm, d) x_c = 6 mm, e) x_c = 12 mm, f) x_c = 18 mm*

The magnetic field distribution can be obtained by the electromagnetic simulation, as shown in Fig. 7. The simulation results indicate that there will be a small amount of magnetic leakage at the top of the coil and the outside of the magnetic steel, respectively. The effect of magnetic concentration is obvious when the two permanent magnets are assembled in reverse,

and the majority of the Lorentz force is generated here. In the whole stroke of VCM, the maximum vector magnetic potential increases slightly from 1.6×10^{-4} WB/m to 1.6171×10^{-4} WB/m; this ensures the stability of the actuation force output of the voice coil motor in the stroke.

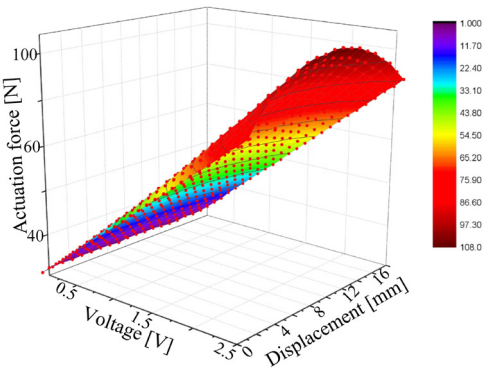

Fig. 8. *Simulation results of VCM actuation force*

Fig. 8 shows the simulation results of the VCM actuation force. The Lorentz force F_e with the variation of parameters (U_c, x_c) has been shown in Fig. 8, of which the coil current ia is determined by coil control voltage U_c and x_c is the coil displacement. With the movement of the coil, the maximum actuation force is generated in the middle section, and the minimum actuation force is generated at both sides of the stroke. The distribution of electromagnetic actuation force is small on both sides and large in the middle section. When the continuous actuation force is 51.5 N, the current is about 1.673 A to 1.804 A.

3.2 Characteristics Analysis of Lever Magnifier

When VCM pushes the lever to drive the spool, the vertical distance between the VCM push rod and the lever fulcrum will change with the rotation of the lever. When the lever is perpendicular to

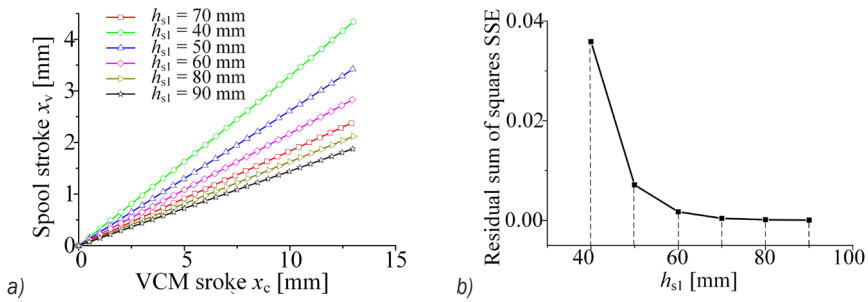

Fig. 9. *Relationship between a) VCM stroke and spool stroke; and b) residual sum of squares*

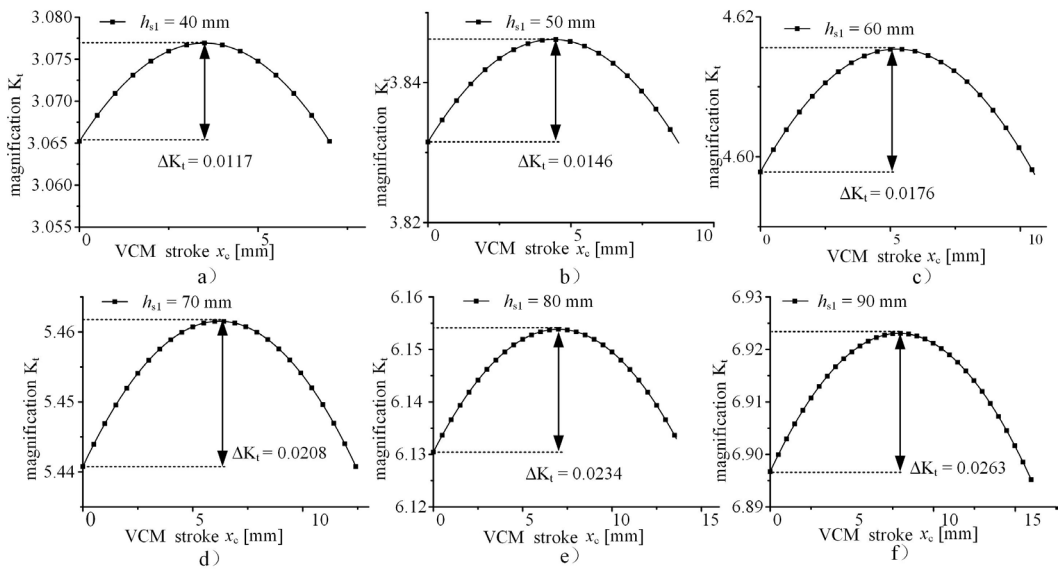

Fig. 10. *Relationship between VCM stroke and magnification; a) h_{s1} = 40 mm, b) h_{s1} = 50 mm, c) h_{s1} = 60 mm, a) h_{s1} = 70 mm, a) h_{s1} = 80 mm, a) h_{s1} = 90 mm*

the horizontal direction, the magnification is the maximum. The variation of magnification will lead to the non-linearity of actuation force and stroke that acts on the spool. Therefore, it is necessary to select the reasonable distance h_{s1} to obtain the linear output performance.

Fig. 9a shows the relationship between VCM stroke and spool stroke when h_{s1} is 40 mm to 90 mm. Fig. 9b is the residual sum of squares (SSE) of the spool stroke in Fig. 9a. With the increase of h_{s1}, SSE decreases gradually. When h_{s1} = 70 mm, a good linear relationship can be obtained. The magnification is between 5.44 and 5.46, and the fluctuation amplitude of magnification is 0.0208, as shown in Fig. 10.

The results show that with the increase of amplification, the amplification fluctuation (ΔK_t is the amplification fluctuation, as shown in Fig. 10) will gradually increase from 0.0117 to 0.0263. Based on the comprehensive comparison and analysis, the optimized value of h_{s1} is 70 mm. and the optimal magnification can be obtained.

4 EXPERIMENTS AND DISCUSSION

A prototype of the water hydraulic proportional valve is developed. The dynamic performance test rig of the valve and VCM have been built, respectively. The dynamic and static performances of VCM and the valve are tested.

4.1 Experimental Study on the Performance of VCM

As shown in Fig. 11a, the actuation force test rig of VCM is mainly composed of support frame, force sensor, displacement sensor, step motor, ball screw, adjustable linear power supply, computer, etc. Fig. 11b shows the schematic diagram of the test system. The industrial computer sends control commands to the stepper motor driver and VCM linear driver through the acquisition card, respectively. The stepper motor drives the linear motion platform to move with VCM through the ball screw. The force sensor is fixed on the base and remains stationary. Therefore, by moving the linear motion platform and adjusting the control signal, the VCM actuation force under different stroke can be tested. The displacement sensor acquisitions the displacement signal, and the force sensor records the VCM actuation force signal every 1 mm interval.

The results presented in Figs. 12 and 13 show the actual test results of VCM actuation force and the difference between simulation and test results. With the movement of the coil, the maximum actuation force

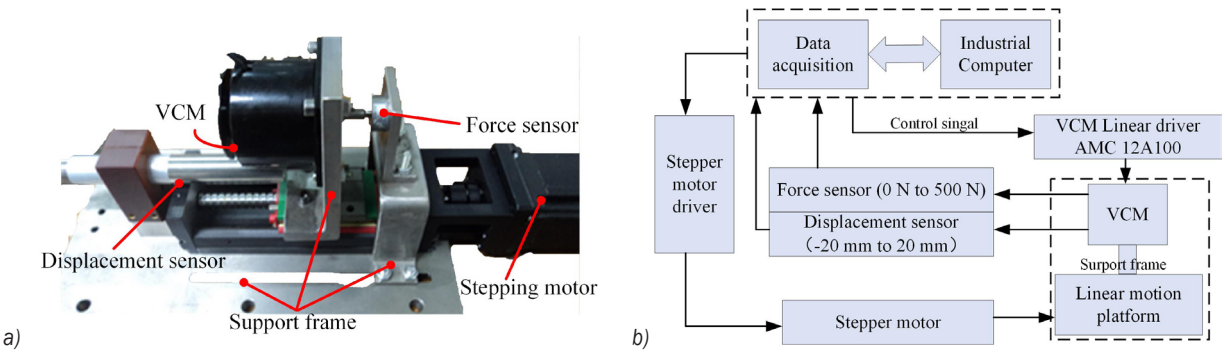

Fig. 11. *VCM actuation force testing rig; a) Testing rig of VCM, b) Schematic diagram of test system*

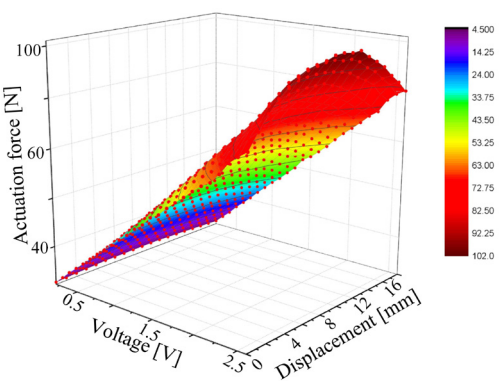

Fig. 12. *VCM actuation force test results*

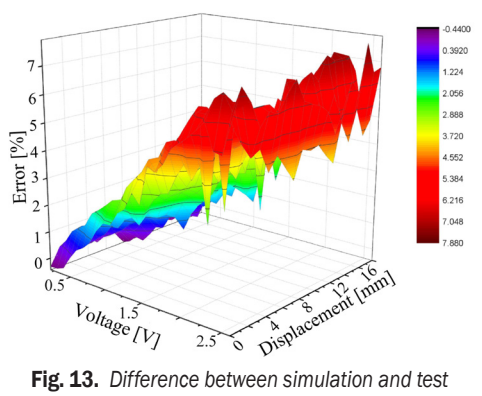

Fig. 13. *Difference between simulation and test of VCM actuation force*

is generated in the middle section, and the minimum actuation force is generated at both sides of the stroke. The distribution of electromagnetic actuation force is small on both sides and large in the middle section. The distribution characteristics of actuation force are essentially consistent with the simulation results. The simulation value is slightly larger than the real test value, and the maximum difference between them is nearly 8 N (the maximum error is 8.4 %). The distribution of error is irregular and significantly fluctuates with the increase of actuation force and displacement. However, in general, the error increases with the increase of actuation force. Both simulation results and test results show that the actuation force decreases in the initial stroke (0 mm to 4 mm) and the end stroke (15 mm to 18 mm). Therefore, the optimal stroke range is 4 mm to 15 mm.

4.2 Experimental Study on Dynamic Performance of the Valve

As shown in Fig. 14, the test system is mainly composed of pump, relief valve, pressure gauges, pressure transducer, displacement transducer, throttle valve, hydraulic multimeter, etc. During the test, the water pump is used to generate rated pressure and rated flow for the prototype valve. The test pressure can be set by adjusting the relief valve.

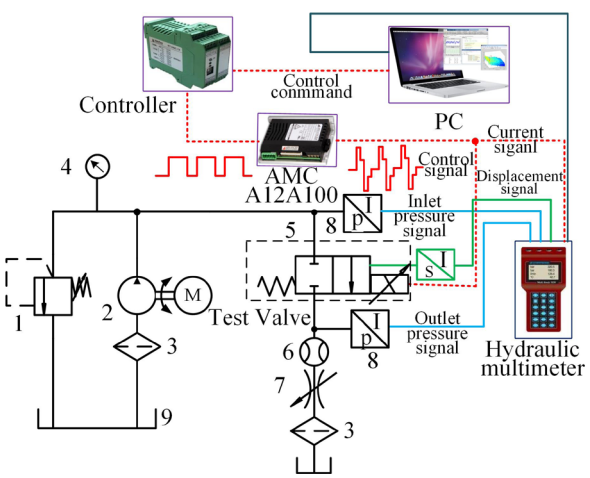

Fig. 14. *Principle of the hydraulic test system; 1. Relief valve, 2. Water pump, 3. Filter, 4. Pressure gage, 5. Water hydraulic valve, 6. Flowmeter, 7. Throttle valve, 8. Pressure transducer, 9. Water tank*

Pressure sensors are installed at the inlet and outlet of the valve. The two different ranges of the pressure sensors are 0 MPa to 20 MPa and 0 MPa to 35 MPa, respectively. The output signals of the pressure sensors are both 4 mA to 20 mA. The range of the eddy current displacement sensor is 0 mm to 2 mm. The output signal of the eddy current displacement sensor is 4 mA to 20 mA. The pressure sensors are used to measure the pressure at the inlet and outlet of the valve. The pressure difference (Δp) can be obtained. The eddy current displacement sensor is installed on the valve and used to measure the valve spool stroke (xv). The PC sends the control commands to the controller. The controller sent control signals into the linear driver (AMC A12A100), and then the control signals will be linearly amplified to drive VCM, in order to control the movement of the valve spool. The displacement signal and pressure signals can be collected in real time with a hydraulic multimeter.

According to the above principle of the hydraulic test system, the test rig is built (as shown in Fig. 15, which is composed of hydraulic power supply, the valve test bench, DC power supply and electrical control system. The linear DC power supplies power to the controller, VCM and sensors. The electric control system realizes the closed-loop control position.

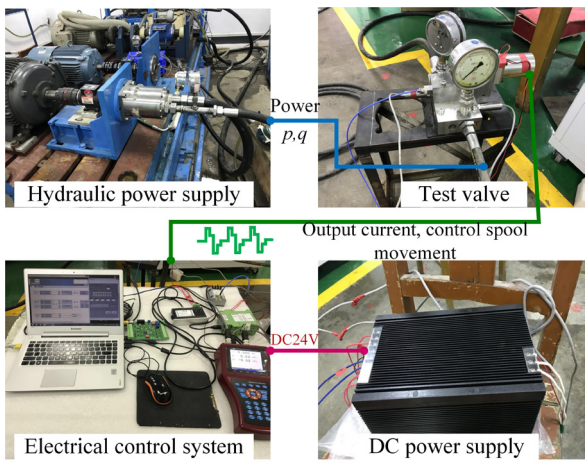

Fig. 15. *The valve dynamic performance test system*

As shown in Fig. 16, the step response (the spool displacement of 1.0 mm, 0.5 mm and 0.1 mm) is compared with the corresponding simulation results. The simulation results show that the step response adjusting time of the valve is about 28 ms and the maximum overshoot is about 5 %. The step response rise time is about 15 ms. Furthermore, the test results indicate that the adjusting time of the opening process is about 30 ms, and the adjusting time of the closing process is about 35 ms. The test results show that there is no obvious delay in the process of opening and closing. It takes more time for the valve spool to close than to open. The actuation force is provided

by VCM when the valve is opening. As the return spring closes the valve when the VCM returns. This is the main reason for the difference between the opening and closing time. The simulation results are in good agreement with the experimental results. An approximately 10 % overshoot occurs when the spool displacement is 1.0 mm, while there is no overshoot when the spool displacement is 0.5 mm and 0.1 mm. The rising time is about 12 ms to 15 ms. The valve has good dynamic performance, and the valve opening and closing process is controlled smoothly.

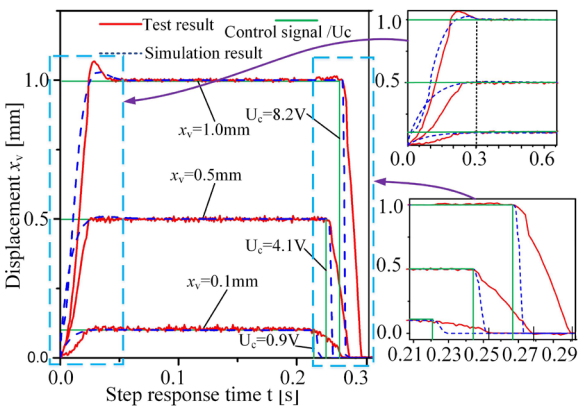

Fig. 16. *Step response test and simulation*

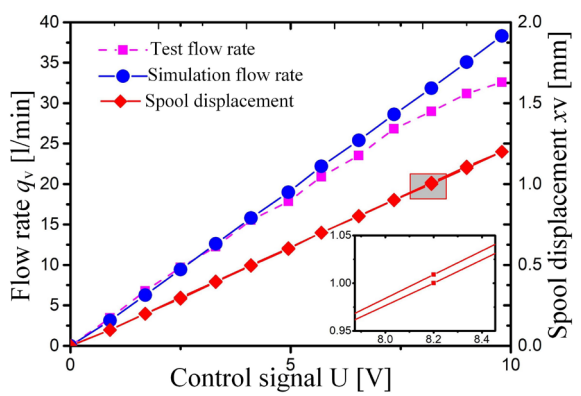

Fig. 17. *Control signal and flow characteristics*

The control signal-spool displacement curve and control signal-flow characteristic curve are shown in Fig. 17. During the test, the inlet pressure of the valve is kept at 1 MPa by adjusting the relief valve. The outlet is connected to the water tank, and the pressure difference between the inlet and outlet of the valve is kept at 1 MPa. The maximum displacement of the valve spool is 1.2 mm in the range of 0 V to 10 V control signal. The control signal has the good linear relationship with the displacement of the valve spool, and the position hysteresis of the valve is less than 1 %. By comparing the experimental flow rate with the simulation results, it can be found that the test flow rate is in good agreement with the simulation flow rate when the control signal is less than 6.5 V. However, the greater the flow rate, the higher the deviation. When the control signal is more than 6.5 V, there is a certain deviation between them, which is mainly caused by the machining error of the valve orifice and the pressure fluctuation of the test system. Generally, the control signal of the valve has a good linear relationship with the flow rate.

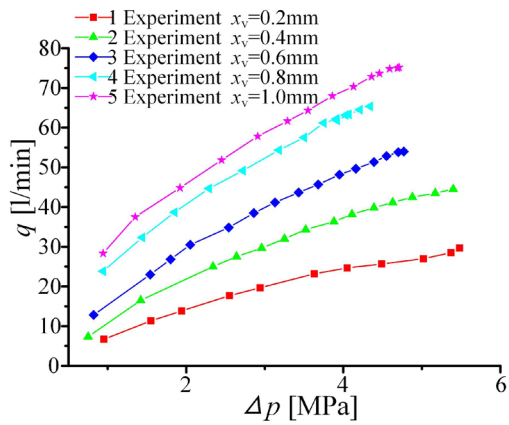

Fig. 18. *q and Δp characteristic*

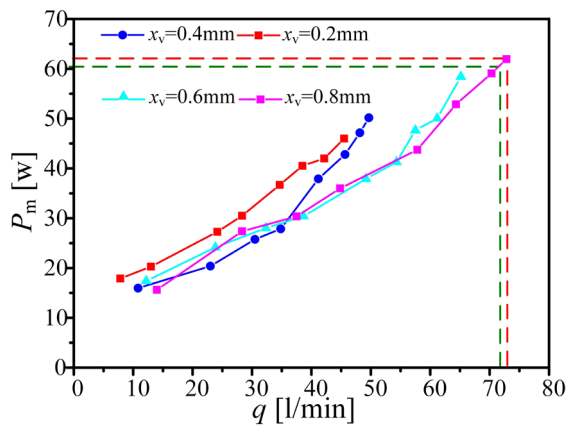

Fig. 19. *The valve input power characteristics*

Fig. 18 shows the pressure difference (Δp) and flow rate (q_v) characteristic under different valve opening (x_v = 0.2 mm, 0.4 mm, 0.6 mm, 0.8 mm, 1.0 mm) in detail. There is irregular change when Δp is over 4 MPa at the valve opening x_v = 0.2mm. This is probably caused by the machining errors at the valve orifice. In general, the results indicate that the Δp *and* q_v characteristics curve is smooth and linear. The valve has good control performance. The relationship between the flow rate and VCM power under different valve opening is shown in Fig. 19. With the increase

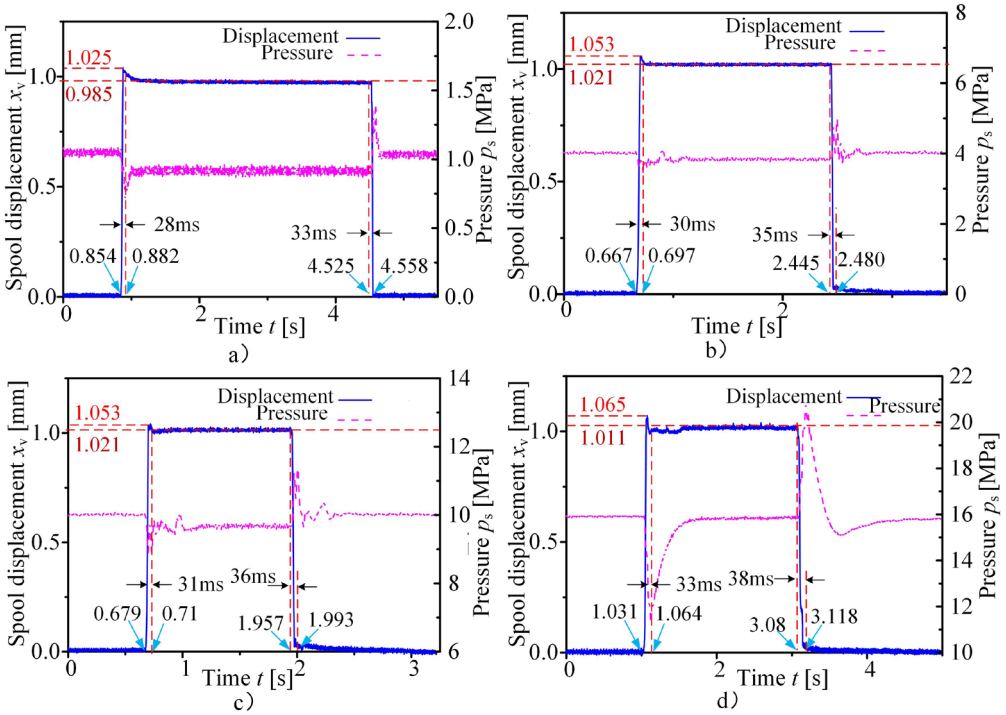

Fig. 20. *Step response under different pressure, a) Δp = 1 MPa, b) Δp = 4 MPa, c) Δp = 10 MPa, d) Δp = 16 MPa*

Table 4. *Step response characteristics comparison*

Manufacturer	MOOG	Tested valve	ATOS	Danfoss
Model	D633/D634	Prototype	QVKZOR-A*-10	VOH30PE
Type	Direct drive servo valve	Proportional valve actuated by VCM	Proportional valve actuated by solenoid	Proportional valve actuated by solenoid
Hydraulic medium	Mineral oil	Water	Mineral oil	Water
Max Pressure	35 MPa	25 MPa	21 MPa	14 MPa
Response time (0 % to 100 % Stroke)	≤12 ms ≤20 ms	30 ms	45 ms	≤150 ms

of the flow rate, the power required to drive the spool will also increase. When the flow rate is 70 l/min, the corresponding VCM power is 60 W, which can meet the requirements of long-term stable and reliable operation of the valve.

The step response test of the valve under different pressures is shown in Fig. 20. During the test, the inlet pressure of the valve is maintained at 1 MPa, 4 MPa, 10 MPa and 16 MPa by adjusting the relief valve, while the outlet is connected with the water tank. Thus, the outlet pressure of the valve is always kept at 0. According to the test results, it can be seen that the maximum overshoot will increase slightly with the increase of the inlet pressure. Nevertheless, the valve can maintain the rapid response performance. The maximum overshoot is approximately 10 %. In general, the adjusting time of the valve is about 30 ms in the opening process and 35 ms in the closing process.

Table 4 shows the comparison between the new water hydraulic valve and the other proportional valves in the market. The step response characteristics of the new valve presented in this paper are better than those of the similar type of oil hydraulic proportional valve. While compared with the servo valve, there is a gap in the dynamic performance. However, compared with the traditional water hydraulic proportional valve (such as Danfoss VOH30PE), the new water hydraulic valve actuated by VCM has better dynamic performance. The results prove that VCM is a good solution instead of solenoids for the hydraulic control valve.

5 CONCLUSIONS

In this study, a water hydraulic proportional valve with fast response is proposed. Given that VCM has the advantages of high speed and high control accuracy, it has been used as the electrical-mechanical conversion device for the valve. Due to the poor viscosity and lubricity of the water medium, the valve will need a large force to push the spool. Thus, a lever amplifier is used to amplify the VCM actuation force. The position feedback closed-loop control has been used to improve the dynamic performance and anti-interference ability of the valve.

A detailed mathematical model of the valve has been developed. The simulation models are established in the MATLAB/Simulink and Maxwell 3D platform, respectively. A comprehensive optimization design method has been proposed. The test rig of the valve and VCM have been built. The dynamic and static performances of VCM and the valve have been tested. Both the VCM actuation force test and simulation results show that the optimal stroke range is 4 mm to 15 mm. According to the dynamic response test, the maximum overshoot of the valve is approximately 10 %, the adjusting time is about 30 ms in the opening process, and 35 ms in the closing process. The test results prove that the valve can maintain a fast response speed under different pressures. Compared with the traditional water hydraulic proportional valve, the new water hydraulic valve actuated by VCM significantly improved the dynamic performance. VCM is a good solution instead of solenoids for the water hydraulic proportional valve. The water hydraulic proportional valve designed in this paper has good static and dynamic control performance.

6 ACKNOWLEDGEMENTS

This work was supported by the National Key R&D Program of China (2018YFB2004001). Project 2662019QD023 supported Fundamental Research Funds for the Central Universities.

7 REFERENCES

[1] Liao, Y.Y., Lian Z.S., Feng J.L., Yuan, H.B., Zhao, R.H. (2018). Effects of multiple factors on water hammer induced by a large flow directional valve. *Strojniški vestnik - Journal of Mechanical Engineering*, vol. 64, no. 5, p. 329-338, **DOI:10.5545/sv-jme.2017.5109**.

[2] Tandon, S., Divi, S., Muglia, M., Vermillion, C., Mazzoleni, A. (2019). Modeling and dynamic analysis of a mobile underwater turbine system for harvesting marine hydrokinetic energy. *Ocean Engineering*, vol. 187, art. ID. 106069, **DOI:10.1016/j.oceaneng.2019.05.051**.

[3] Woodacre, J.K., Bauer, R.J., Irani, R. (2018). Hydraulic valve-based active-heave compensation using a model-predictive controller with non-linear valve compensations. *Ocean Engineering*, vol. 152, p. 47-56, **DOI:10.1016/j.oceaneng.2018.01.030**.

[4] Liao, Y.Y., Yuan, H.B., Lian, Z.S., Feng, J.L., Guo, Y.C. (2015). Research and analysis of the hysteresis characteristics of a large flow directional valve. *Strojniški vestnik - Journal of Mechanical Engineering*, vol. 61, no. 6, p. 355-364, **DOI:10.5545/sv-jme.2015.2487**.

[5] Han, M.X., Liu, Y.S., Wu, D.F., Zhao, X.F., Tan, H.J. (2017). A numerical investigation in characteristics of flow force under cavitation state inside the water hydraulic poppet valves. *International Journal of Heat and Mass Transfer*, vol. 111, p. 1-16, **DOI:10.1016/j.ijheatmasstransfer.2017.03.100**.

[6] Majdic, F., Pezdirnik, J. (2010). Oil- and water-based continuous control valve. *Industrial Lubrication and Tribology*, vol. 62, no. 3, p. 136-143, **DOI:10.1108/00368791011034511**.

[7] Han, M.X., Liu, Y.S., Zheng K., Ding, Y.C., Wu, D.F. (2020). Investigation on the modeling and dynamic characteristics of a fast-response and large-flow water hydraulic proportional cartridge valve. *Proceedings of the Institution of Mechanical Engineers, Part C: Journal of Mechanical Engineering Science*, vol. 234, no. 22, p. 4415-4432, **DOI:10.1177/0954406220922860**.

[8] Zhu, K.W., Gu, L.Y., Chen, Y.J., Li, W. (2012). High speed on/off valve control hydraulic propeller. *Chinese Journal of Mechanical Engineering*, vol. 25, no. 3, p. 463-473, **DOI:10.3901/CJME.2012.03.463**.

[9] Mahrenholz, J., Lumkes, J.J. (2010). Analytical coupled modeling and model validation of hydraulic on/off valves. *Journal of Dynamics Systems, Measurement, and Control*, vol. 132, no. 1, p. 1-10, **DOI:10.1115/1.4000072**.

[10] Park, S.-H., Kitagawa, A., Kawashima, M., (2004). Water hydraulic high-speed solenoid valve. Part I: development and static behavior. *Proceedings of the Institution of Mechanical Engineers, Part I: Journal of Systems and Control Engineering*, vol. 218, no. 5, p. 399-499, **DOI:10.1243/0959651041568560**.

[11] Park, S.-H. (2009). Development of a proportional poppet-type water hydraulic valve. *Proceedings of the Institution of Mechanical Engineers, Part C: Journal of Mechanical Engineering Science*, vol. 223, no. 9, p. 2099-2107, **DOI:10.1243/09544062JMES1380**.

[12] Roberts, D.C., Li, H., Steyn, J.L., Yaglioglu, O., Spearing, S.M., Schmidt, M.A., Hagood, N.W. (2003). A piezoelectric microvalve for compact high-frequency, high-differential pressure hydraulic micropumping systems. *Journal of Microelectromechanical Systems*, vol. 12, no. 1, p. 81-92, **DOI:10.1109/JMEMS.2002.807471**.

[13] Rogge, T., Rummler, Z., Schomburg, W.K. (2004). Polymer micro-valve with a hydraulic piezo-drive fabricated by the AMANDA process. *Sensors and Actuators A: Physical*, vol. 110, no. 1-3, p. 206-212, **DOI:10.1016/j.sna.2003.10.056**.

[14] Ahn, D.H., Hong, D.P., Gweon, D.G. (2014). Design of a high force voice coil motor. *Applied Mechanics and Materials,*

vol. 483, p. 559-562, **DOI:10.4028/www.scientific.net/AMM.483.559**.

[15] Li, B.R., Gao, L.L., Yang, G. (2013). Modeling and control of a novel high-pressure pneumatic servo valve direct-driven by voice coil motor. *Journal of Dynamic Systems, Measurement, and Control*, vol. 135, no. 1, p. 1-5, **DOI:10.1115/1.4007702**.

[16] Li, B.R., Gao, L.L., Yang, G. (2013). Evaluation and compensation of steady gas flow force on the high-pressure electro-pneumatic servo valve direct-driven by voice coil motor. *Energy Conversion and Management*, vol. 67, p. 92-102, **DOI:10.1016/j.enconman.2012.11.004**.

[17] Zhang, Z.M., Gong, Y.J. Hou, J.Y., Wu, H.P. (2014). Simulation on linear-motor-driven water hydraulic reciprocating plunger pump. *Advanced Materials Research*, vol. 842, p. 530-535, **DOI:10.4028/www.scientific.net/AMR.842.530**.

[18] Liu, W., Wei, J.H., Fang, J.H., Li, S.Z. (2015). Hydraulic-feedback proportional valve design for construction machinery. *Proceedings of the Institution of Mechanical Engineers, Part C: Journal of Mechanical Engineering Science*, vol. 229, no. 17, p. 3162-3178, **DOI:10.1177/0954406214568822**.

[19] Filo, G., Lisowski, E., Kwiatkowski, D., Rajda J., (2019). Numerical and experimental study of a novel valve using the return stream energy to adjust the speed of a hydraulic actuator. *Strojniški vestnik - Journal of Mechanical Engineering*, vol. 65, no. 2, p. 103-112, **DOI:10.5545/sv-jme.2018.5823**.

[20] Xu, Y. L., Nie, H.W., Zhao, H.L., Liu, J. (2020). Mathematical modelling and simulation of a novel hydraulic variable valve timing system. *International Journal of Simulation Modelling,* vol. 19, no. 2, p. 303-312, **DOI:10.2507/IJSIMM19-2-C06**.

[21] Simic, M., Herakovic, N. (2015). Reduction of the flow forces in a small hydraulic seat valve as alternative approach to improve the valve characteristics. *Energy Conversion and Management,* vol. 89, p. 708-718, **DOI:10.1016/j.enconman.2014.10.037**.

[22] Karanović, V., Jocanović, M., Baloš, S., Knežević, D., Mačužić, I. (2019). Impact of contaminated fluid on the working performances of hydraulic directional control valves. *Strojniški vestnik - Journal of Mechanical Engineering*, vol. 65, no. 3, p. 139-147, **DOI:10.5545/sv-jme.2018.5856**.